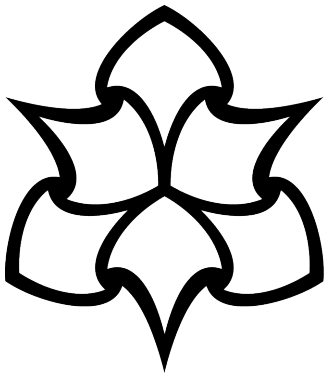

Classification of fentanyl analogues through Principal Component Analysis (PCA) and Hierarchical Clustering of GC-MS data

Nicolas Gilbert[1,2*], Ryan E. Mewis[1,2] and Oliver B. Sutcliffe[1,2*]

[1]MANchester DRug Analysis & Knowledge Exchange (MANDRAKE), Manchester Metropolitan University, Chester Street, Manchester, UK. M1 5GD

[2]Faculty of Science and Engineering, Department of Natural Sciences, Manchester Metropolitan University, Chester Street, Manchester, UK. M1 5GD

[*]Corresponding author(s): Mr. Nicolas Gilbert (email. nicolas.gilbert@mmu.ac.uk); Dr Oliver B Sutcliffe (email. o.sutcliffe@mmu.ac.uk; Tel. +44 (0)161 247 1531).

Highlights

- PCA – hierarchical clustering model was built from fentanyl analogues EI-MS data.
- Model allows classification of 67 analogues with 91% accuracy.
- Classification is based on position of modification and moiety introduced.
- Method can assist structural elucidation of novel analogues.

Abstract

The emergence of a wide variety of fentanyl analogues has become a problem for the identification of seized drug samples. While chemical databases are largely reactive to the emergence of new analogues, efforts should focus on the development of predictive models which can discern how new analogues differ from the parent drug. Principal component analysis (PCA) was performed on mass spectral data from 54 fentanyl analogues. Hierarchical clustering was used to group these analogues into meaningful classes. The model was able to classify 67 analogues not previously included in the model with high accuracy, based on the nature and position of the chemical modification.

Keywords: Forensic, illicit drugs, fentanyl analogues; GC-MS; principal component analysis; hierarchical clustering

1. Introduction

Abuse of the synthetic opioid fentanyl started in the 1980s and has grown ever since into a serious threat for public health. [1-4] A marked increase in lethal overdoses linked to fentanyl and its analogues has been observed in the last decade. Although it is most prevalent in the United States, fentanyl has been reported in fatalities in Canada, Australia and Europe, making it a global issue. [5-9] The increase in fentanyl abuse has been associated with the emergence of a large variety of fentanyl analogues: between 2013 and 2019, the United Nations Office on Drugs and Crime (UNODC) reported more than 75 New Psychoactive Substances with opioid effect (including fentanyl analogues) in its Early Warning Advisory and this number keeps growing. [10]

This quick emergence of synthetic analogues of controlled drugs constitutes a challenge for their identification because of the time it takes before extensive chemical characterisation of these analogues is disseminated in academic journals or specialised databases. [3, 11] The most commonly modified positions of fentanyl are highlighted in **Figure 1**. Permutations of these modifications are easily introduced in novel analogues by changing one or more synthetic precursors. While chemical databases of controlled drugs are reactive to the emergence of new analogues, proactive solutions should be considered to quickly identify future analogues. Efforts should thus focus on the development of predictive models which, when confronted with unknown drug analogues not present in a database, can still discern in what ways the analogues differ from the parent drug.

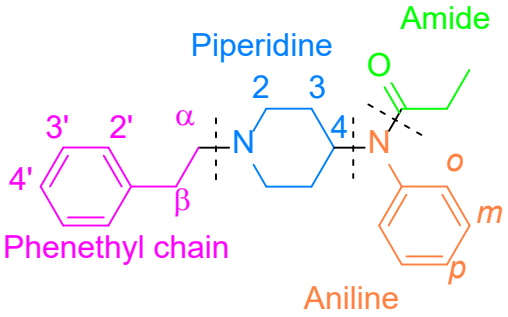

Figure 1. Commonly modified positions in fentanyl.

Mass spectrometry data appears to be the ideal technique for this purpose, partly because of its widespread use: multiple gas chromatography-mass spectrometry (GC-MS) methods have been reported for the detection of fentanyl and its derivatives. [12-15] GC-MS also allows the separation of multicomponent mixtures, which facilitates the detection of fentanyl in mixed samples. Moreover, m/z ions are indicative of specific modifications and their position on the molecule. How easily characteristic fragments can be identified by an experimenter can be greatly impacted by the complexity of mass spectra. Techniques based on dimensionality reduction, such as principal component analysis (PCA), are therefore perfectly suited for this type of analysis and can highlight unsuspected trends in spectral data. New observations can also be projected onto the PCA model to see how they relate to known analogues. [16]

Multivariate analysis has been used to determine the synthetic route used to manufacture fentanyl samples based on an inventory of compounds detected by GC-MS, LC-MS/MS and ICP-MS. [17] It has also been used to differentiate fentanyl analogues from other drugs of abuse, based on their Raman spectra. [18] Principal component analysis has been used to highlight mass spectral differences between synthetic drug analogues, which tend to produce different ion ratios, and in one case to discriminate regioisomers of fluorofentanyl. [19-23] Recently, spectral similarity mapping was applied to group fentanyl analogue mass spectra based on their match factors. [24] Clustering mostly arose based on the number of peaks that shifted (0, 1 or 3) between an analogue and fentanyl, an indicator of the position of a structural modification.

This paper proposes a principal component analysis model which organises data based on the presence of specific m/z ions. Coupled with hierarchical clustering, this allows the reliable classification of fentanyl analogues based on specific structural modifications. The model was built using the mass spectra of 54 analogues available in the SWGDRUG spectral library or acquired from in-house standards. Model evaluation was performed using 67 analogues not previously included in the model. This demonstrates that PCA allows clustering based not only on the structural position of a modification, but also on the moiety introduced. The model can be used to classify novel, emerging fentanyl analogues to assist in their structural elucidation.

2. Material and methods

2.1 Analytes and gas chromatography-mass spectrometry (GC-MS) data acquisition

A full list of the fentanyl analogues utilised in this study is provided in **Table S1** (see Supplementary Information). Mass spectra for compounds **1-7**, **20-21**, **24-35**, **39-43**, **52-54**, **56-60**, **62-63**, **77**, **87**, **92-99** and **111** were acquired from standards synthesised in-house, in accordance with Manchester Metropolitan University's controlled drug's license (Ref. No. 423023) requirements and agreed procedures. Synthetic procedures were adapted from the literature and are reported in the Supplementary Information. [25-27] Spectra were acquired using an Agilent 7890B GC and a MS5977B mass selective detector (Agilent Technologies, Wokingham, UK). The mass spectrometer was operated in the electron ionization mode at 70 eV. Separation was achieved with a capillary column (HP-5MS, 30 m length, 0.25 mm i.d., 0.25 µm film thickness) with helium as the carrier gas at a constant flow rate of 1.2 mL/min. A 2 µL aliquot of the samples was injected with a split ratio of 50:1. The injector and the GC interface temperatures were both maintained at 280 °C and 290 °C respectively. The following oven temperature programme was used: 50-290 °C at 30 °C/min, hold for 8 minutes. The MS source and quadrupole temperatures were set at 230 °C and 150 °C respectively. Scan spectra were obtained between 41-550 amu. The remaining EI mass spectra were taken from the SWGDRUG spectral library (version 3.7, released June 4th, 2020). [28]

All mass spectra were extracted in .csv format. Only peaks between m/z = 41 and 352 were retained and rounded to the nearest mass unit, and the dataset was zero-filled. Relative intensities were calculated, with the base peak normalized to an intensity of 1. The resulting dataset was imported into R statistical computing software (version 3.6.3). The software implementation that generates mass spectral similarity mappings of unknowns against a library of fentanyl analogue spectra (.csv format) is provided as Supplementary Information and available on Github (https://github.com/Nicolas-Gilbert/Fentanyl-PCA-HC).

2.2 Principal component analysis (PCA)

Compounds were separated into nine generic structural classes (see Supplementary Information, Table S2). Approximately half the compounds in each class (at least three) were selected randomly to build the model. These classes did not inform hierarchical clustering but served to have an even

representation of possible structural classes. In total, 54 analogues were used to build the model. Variables (m/z ions) with a variance below 0.0001 were excluded as an initial clean-up, which reduced the dataset to 176 variables. This removed ions absent from all analogues, or ions that occurred very strongly in only one (or very few) compounds. Higher variance thresholds were tested and led to a loss of valuable information when building the model (i.e. poor separation of structural classes). Principal component analysis was performed with mean centering and data scaling, using the PCA function from the FactoMineR package (version 2.2). [29] Data visualisation was performed using the factoextra package (version 1.0.7). [30]

2.3 Hierarchical clustering

Hierarchical clustering was performed using the HCPC function from the FactoMineR package. This function uses inertia as a measure of inter- and intra-class variability. The ascendant hierarchical classification starts with as many classes as there are individuals, then groups classes in a way that maximises inter-class inertia (or intervariability). [29, 31] Grouping classes together can only lead to a decrease in the inter-class inertia, and the following equation (**Eqn. 1**) describes how the inertia of two classes a and b decreases when they are grouped together:

$$\text{Inertia}(a) + \text{Inertia}(b) = \text{Inertia}(a \cup b) - \frac{m_a m_b}{m_a + m_b} d^2(a,b) \qquad \textbf{Eqn 1.}$$

where m_a and m_b are the numbers of individuals in classes a and b and $d^2(a,b)$ is the squared distance between the centers of gravity of a and b. When a and b are grouped together, inertia is decreased by a value proportional to the distance between the two classes, weighted by the number of individuals in each class. The HCPC function uses Ward's method, which aims to make the negative term of this equation as small as possible; it groups the two classes that lead to the smallest loss of inertia, then the next smallest loss, and so forth until this iterative process builds a full dendrogram. [29, 31] In the resulting dendrogram, when two classes are grouped together, the height of the branch represents the resulting loss of inertia. The user must specify the number of expected classes, but the nature of these classes arises entirely from the proximity of individuals in the dendrogram. The gap statistic method developed by Tibshirani et al. was also explored as a criterion for determining the number of clusters. [32] Cluster quality was evaluated using the

silhouette coefficient (S_i) method from factoextra, is defined in the following equation (**Eqn. 2**). [31, 33]:

$$S_i = \frac{(b_i - a_i)}{\max(a_i, b_i)} \qquad \textbf{Eqn 2.}$$

For each individual i, the average dissimilarity a_i between it and other members of its cluster is calculated. Then, the average dissimilarity between i and every other cluster is calculated; the smallest of these, i.e. the dissimilarity between i and its neighbour cluster, is noted b_i. This coefficient can take values between -1 and 1 and measures the quality of clustering for each object. A coefficient near 1 means an object clusters almost perfectly, 0 means it lies between two clusters and a negative value indicates that an individual is likely in the wrong cluster.

2.4 Model evaluation

The spectra of 67 compounds, which were not included when building the model, were used for evaluation. These data were imported into R and the same m/z ions were removed as in the initial clean-up. Two classification criteria were compared based on their accuracy. Firstly, the centroid of each cluster was calculated, and test samples were classified based on the closest centroid. In contrast, test samples were also classified into the cluster of the closest individual, or nearest neighbour.

3. Results and discussion

3.1 Principal component analysis (PCA)

The model data consisted of 54 observations (compounds) of 176 variables (m/z ions). Because of the high number of variables, PCA was used to reduce the number of dimensions to a small number of principal components (PCs). Before selecting how many PCs should be retained, the information represented by each of the first principal components was examined.

Figure 2 shows a projection of the model compounds on PCs 1 and 2 as well as the corresponding correlation circle. In the latter, m/z ions are coloured based on their squared cosine (cos^2) values, which correspond to the squared cosine of the angle made between a variable and the PC axis. [16] The cos^2 value correlates to the projection of a variable on a given PC. Mass ions with a high cos^2

are best represented by a given PC and, ultimately, are most characteristic of compounds projected in a given direction. For example, N-benzyl analogues gather in the lower left quadrant (**Figure 2a**) and are most strongly characterised by m/z = 82, 91, 172, 173 and 174 (**Figure 2b**). These are piperidine or tropylium (m/z = 91) fragments which arise more strongly in N-benzyl than N-phenethyl derivatives. [34] The structure of these ions will be further discussed in Section 3.2.

PC1, on its positive axis, appears strongly characteristic of fluorinated derivatives, especially those bearing a propionylamide chain (**Figure 2a**). It also separates 3-fluoro- and methoxyaniline derivatives from the bulk, to a lesser extent. Positive values of PC2 characterises most amide derivatives and fluorophenethyl- compounds, while negative values are representative of chloro- and fluoro-aniline containing compounds. A combination of PC1 and PC2 separates N-benzyl derivatives from the rest of compounds. Projections on PCs 3 to 6 are reported shown in the Supplementary Information (see **Figures S1** and **S2**). PC3 characterises chloro-aniline compounds, and PC4 is representative of methoxy-aniline compounds. Finally, PC5 serves to discriminate 3-fluoro compounds from the bulk. PC6 does not appear to contribute significantly to clustering, showing a rather even distribution of compounds along its axis. PCs beyond PC6 explain decreasing proportions of the total variance and are unlikely to contribute to the model. Therefore, the first five PCs were retained, which explain 40.0% of the total variance in the data. A Scree plot of the eigenvalues of the first PCs is included in the Supplementary Information (**Figure S3**). The relatively low variance explained by the first PCs may be due to the nature of the data, and the overall variability of m/z ions across so many different types of analogues: much of the variance may remain in further PCs. A recent study using mass spectral data from synthetic phenethylamines and tryptamines obtained similarly low values of variance explained by the first PCs. [12] In this case as well, PCs were selected based on their importance in separating structural classes, rather than on a variance criterion.

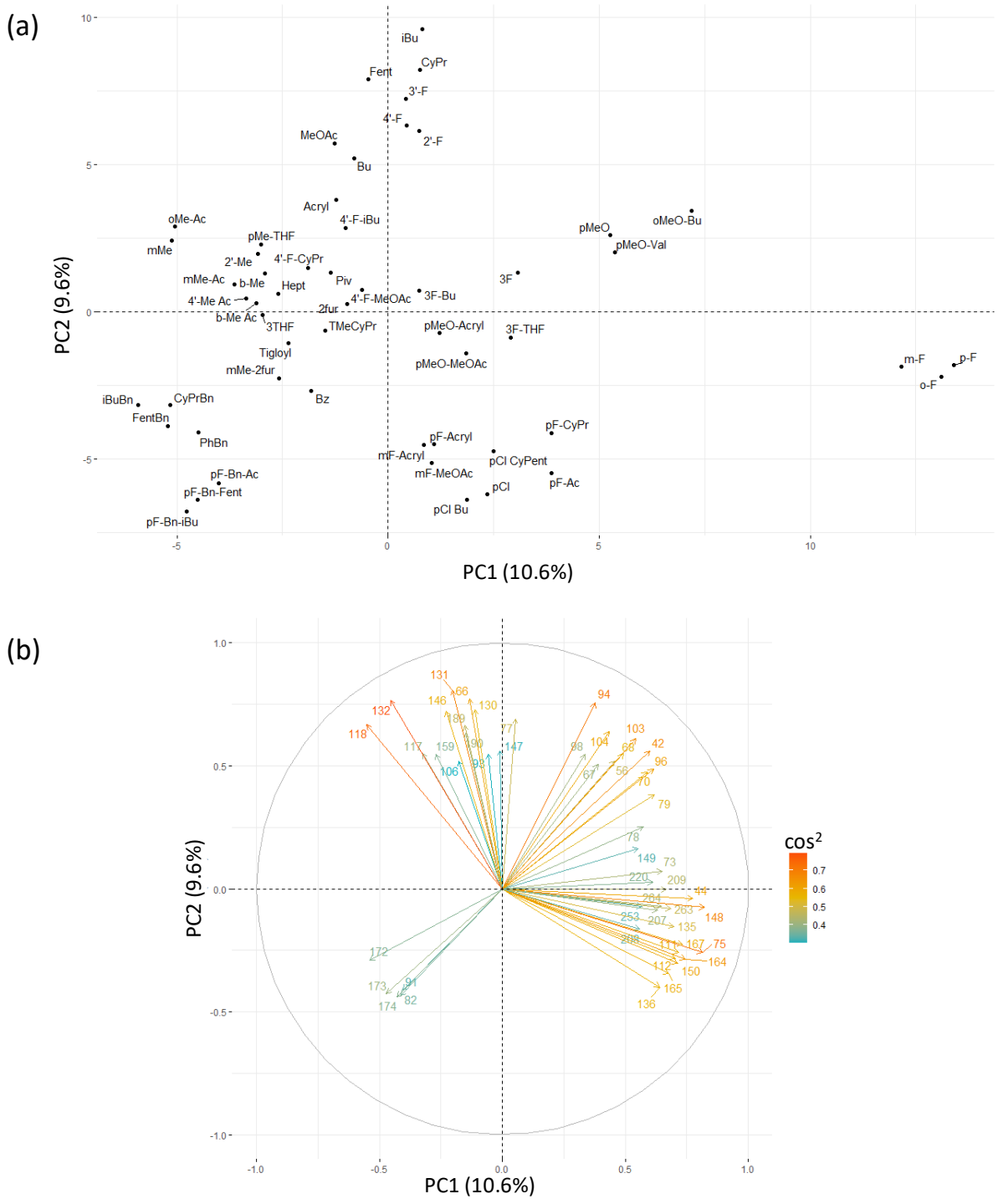

Figure 2. (a) Projection of model fentanyl analogues on principal components PC1 and PC2; (b) Correlation circle of m/z values projected on principal components PC1 and PC2, coloured according to $\cos^2$ values.

3.2 Hierarchical clustering

As described in Section 2.3, a hierarchical clustering dendrogram was built from the PCA data (see **Figure 3** for an example). Classes generated through hierarchical clustering are defined by "cutting" the dendrogram at an appropriate level. Therefore, the number of classes can be defined by the experimenter, but the composition of these classes arises solely from the clustering algorithm and the inertia criterion described in Section 2.3.

The hierarchical clustering algorithm in FactoMineR automatically suggested seven classes in this case. By working its way from the top of the dendrogram, it calculated the relative gain of inertia of each grouping and suggested the grouping with the highest relative gain. In contrast, the gap statistic method suggested using eleven clusters. Both resulting dendrograms are shown in the Supplementary Information (Figure S4). Looking at Figure **S4a** (k = 7), clusters 5 and 7, which are the most heterogeneous according to their branch height, make little sense. Cluster 5 includes fluorophenethyl derivatives (**33-35**) with non-fluorinated analogues (**27-32**), while cluster 7 includes N-benzyl derivatives (**1-7**) with fluoroaniline analogues (**36-40**), and each cluster could arguably be cut in half. In contrast, the partition obtained from the gap statistic, shown in Figure **S4b** (k = 11), contains too many groups. Clusters 1 and 2 separate two methoxyaniline derivatives (para-methoxyacrylfentanyl (**47**) and para-methoxymethoxyacetylfentanyl (**48**)) from the rest, which does not seem to be a useful distinction. Cluster 8 is composed of methylaniline derivatives (**8-9**, **14**), while closely related compounds meta-methylacetylfentanyl (**10**) and meta-methyl-2-furanylfentanyl (**18**) fall in cluster 9. In fact, cluster 9 includes analogues which remain close to the center of the PCA space, compounds which could potentially be resolved from the rest of the group by subtle differences in their mass spectra, but which explain a low percentage of the variance in this dataset.

Based on these observations, partitions with k = 7 and 11 clusters inadequately represent the structural classes present in the dataset, as outlined in **Table S2**, and an intermediate partition with 9 clusters would be best. This partition is called "Classifier 1" and is shown in **Figure 3**. **Figure 4** shows the same partition in the PCA space, on the PC1-PC2 plane. Although PCs 3-5 are omitted, they also contribute to the clustering. A detailed list of the compounds in each cluster is reported in Table 1.

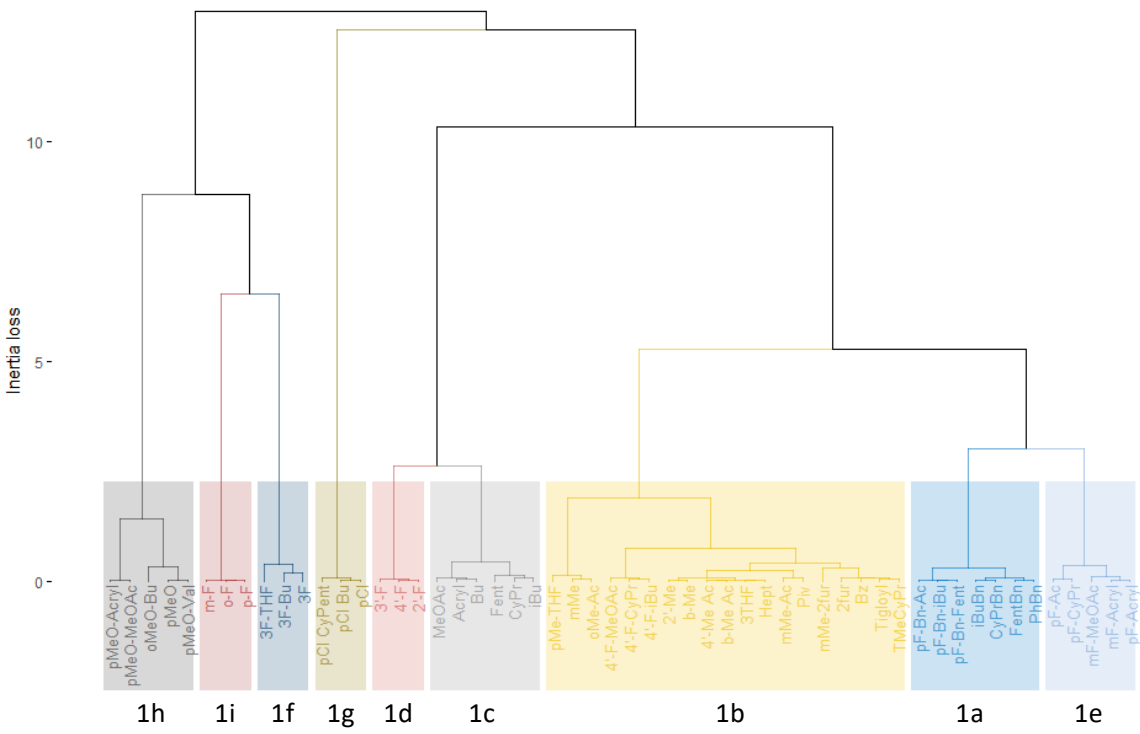

Figure 3. Classifier 1 dendrogram created from the hierarchical clustering of fentanyl analogues. Note: The vertical axis represents the loss of inertia caused by each grouping.

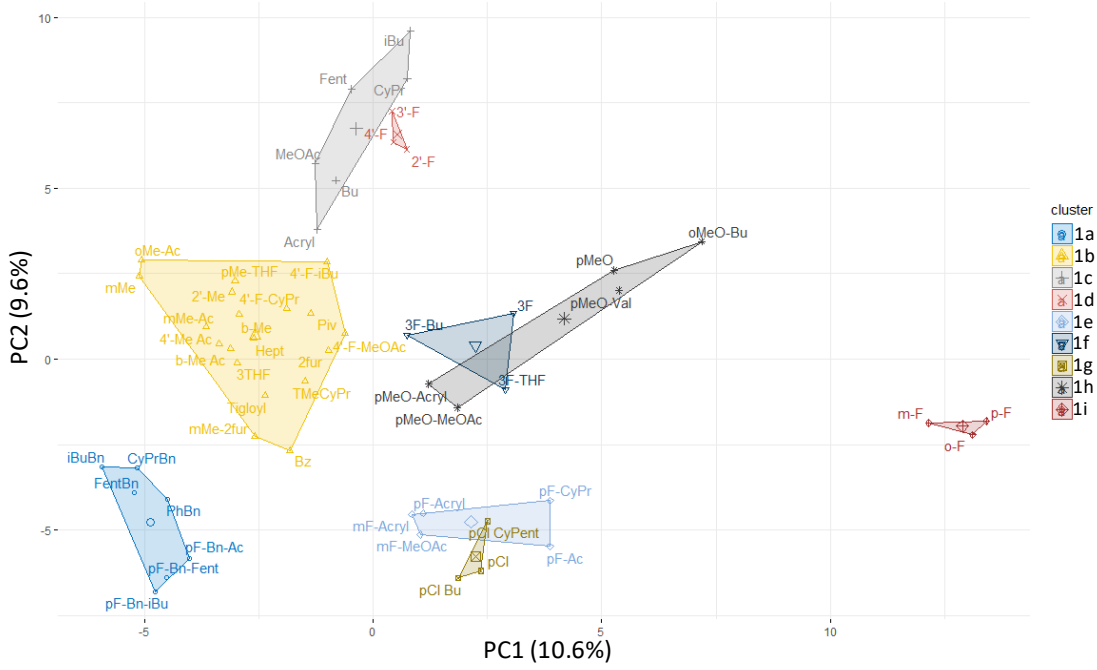

Figure 4. Hierarchical clustering (Classifier 1) shown on the PC1-PC2 plane. Note: PCs 3-5 are not shown but also contribute to the clustering.

Table 1. Individuals in each cluster of Classifier 1.

Cluster		Fentanyl analogue	Abbreviation	Nº
1a	N-Benzyl-	Isobutyryl N-benzyl-	iBuBn	**1**
		N-Benzyl-	FentBn	**2**
		Cyclopropyl-N-benzyl-	CyPrBn	**3**
		para-Fluoro-isobutyryl-N-benzyl-	pF-Bn-iBu	**4**
		para-Fluoro-N-benzyl-	pF-Bn-Fent	**5**
		Phenyl-N-benzyl-	PhBn	**6**
		para-Fluoro-acetyl-N-benzyl-	pF-Bn-Ac	**7**
1b	Inconclusive	meta-Methyl-	mMe	**8**
		ortho-Methyl-acetyl-	oMe-Ac	**9**
		meta-Methyl-acetyl-	mMe-Ac	**10**
		4'-Methyl-acetyl-	4'-Me Ac	**11**
		β-Methyl-acetyl-	b-Me Ac	**12**
		2'-Methyl-	2'-Me	**13**
		para-Methyl-tetrahydrofuranyl-	pMe-THF	**14**
		Tetrahydrofuranyl- (3-isomer)	3THF	**15**
		β-Methyl-	b-Me	**16**
		Heptanoyl-	Hept	**17**
		meta-Methyl-furanyl-	mMe-2fur	**18**
		((E)-2-Methyl-2-butenoyl)-	Tigloyl	**19**
		4'-Fluoro-cyclopropyl-	4'-F-CyPr	**20**
		Benzoyl- (phenyl)	Bz	**21**
		2,2,3,3-Tetramethylcyclopropyl-	TMeCyPr	**22**
		2,2-dimethylpropanoyl-	Piv	**23**
		4'-Fluoro-butyryl-	4'-F-Bu	**24**
		Furanyl-	2-fur	**25**
		4'-Fluoro-methoxyacetyl-	4'-F-MeOAc	**26**
1c	Amides	Methoxyacetyl-	MeOAc	**27**

Cluster		Fentanyl analogue	Abbreviation	Nº
1c	Amides	Acryl-	Acryl	**28**
		Butyryl-	Bu	**29**
		Propionyl-	Fent	**30**
		Cyclopropyl-	CyPr	**31**
		Isobutyryl-	iBu	**32**
1d	Fluorophenethyl (Propionyl)	3'-Fluoro-	3'-F	**33**
		4'-Fluoro-	4'-F	**34**
		2'-Fluoro-	2'-F	**35**
1e	Fluoroanilines	meta-Fluoro-acryl-	mF-Acryl	**36**
		meta-Fluoro-methoxyacetyl-	mF-MeOAc	**37**
		para-Fluoro-acryl-	pF-Acryl	**38**
		para-Fluoro-acetyl-	pF-Ac	**39**
		para-Fluoro-cyclopropyl-	pF-CyPr	**40**
1f	3-Fluoro-	3-Fluoro-butyryl-	3F-Bu	**41**
		3-Fluoro-tetrahydrofuranyl-	3F-THF	**42**
		3-Fluoro-	3F	**43**
1g	Chloroanilines	para-Chloro-butyryl-	pCl Bu	**44**
		para-Chloro-	pCl	**45**
		para-Chloro-cyclopentyl-	pCl CyPent	**46**
1h	Methoxyanilines	para-Methoxy-acryl-	pMeO-Acryl	**47**
		para-Methoxy-methoxyacetyl-	pMeO-MeOAc	**48**
		para-Methoxy-	pMeO	**49**
		para-Methoxy-valeryl-	pMeO-Val	**50**
		ortho-Methoxy-butyryl-	oMeO-Bu	**51**
1i	Fluoroanilines (Propionyl)	meta-Fluoro-	m-F	**52**
		ortho-Fluoro-	o-F	**53**
		para-Fluoro-	p-F	**54**

The quality of these clusters was evaluated based on the silhouette coefficient of each individual (**Figure 5**). This coefficient can take values between -1 and 1 and measures the quality of clustering for each object. A coefficient near 1 means an object clusters almost perfectly, 0 means it lies between two clusters and a negative value indicates that an individual is likely in the wrong cluster. The silhouette plot shows that all individuals have a coefficient above 0 and cluster relatively well. The least cohesive cluster appears to be cluster 1b.

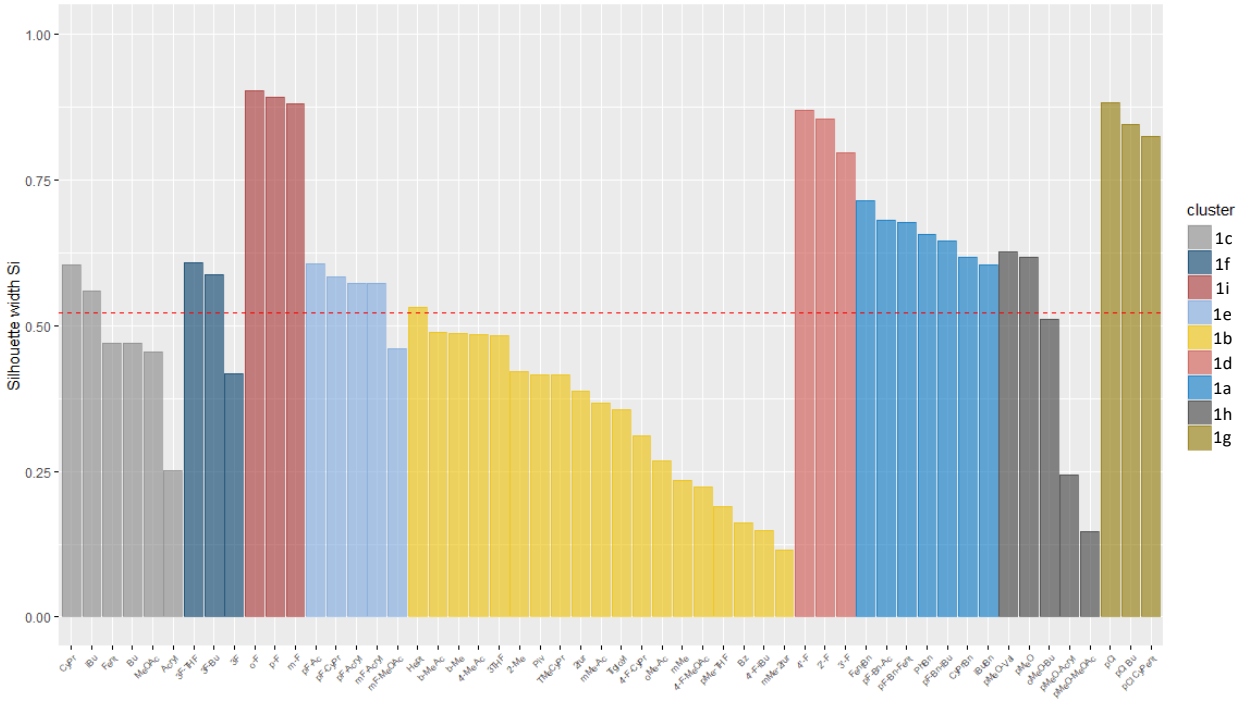

Figure 5. Silhouette coefficients of individuals in Classifier 1. Note: The doted line represents the average silhouette coefficient.

The clusters observed in Classifier 1 mostly correspond to structural classes expected in the dataset (**Table S2**), with some exceptions. 2'-Fluoro-, 3'-fluoro- and 4'-fluorofentanyl (**33-35**; cluster 1d) are separated from 4'-fluorinated compounds which bear different amide chains (**20**, **24**, **26**; cluster 1b). The same goes for ortho-fluoro-, meta-fluoro- and para-fluorofentanyl (**52-54**; cluster 1i) which are separate from other fluoroaniline compounds (cluster 1e). Finally, cluster 1b, includes compounds from multiple structural classes, classed as "inconclusive" by Classifier 1.

Clustering can be better understood by considering the m/z ions which are most characteristic of the individuals in a cluster (see **Table 2**). Ions reported in **Table 2** show a significantly higher intensity in a given cluster than in the whole dataset. The reported p-value shows the probability that an m/z ion does not significantly deviate from a normal distribution; in other words, ions with a low p-value are more likely to be significantly stronger in a cluster. Ions that have a significantly lower mean in a cluster than in the total dataset can also contribute to clustering, but they were omitted from **Table 2** because they are not indicative of the EI-MS fragments shared by members of a class.

Most characteristic ions tend not to include the amide chain, but rather portions of the molecule which are common to all derivatives in a class. For instance, cluster 1a includes N-benzyl derivatives (**1-7**) and is characterised mostly by m/z = 82, 91 and 173, ions which have previously been reported to arise strongly in this class of compounds, and not in traditional N-phenethyl analogues. Cluster 1b includes ions methylated on the aniline ring (m/z = 160, 203) or the phenethyl chain (m/z = 119). As noted before, cluster 1b includes "inconclusive" compounds; it is situated close to the center of the PCA space and is the most heterogeneous cluster. Ions characteristic of cluster 1b also deviate less strongly from the normal distribution than other clusters: the p-value of the most characteristic cluster 1b ion (m/z = 160, p-value = 9.1×10^{-3}) is many orders of magnitude lower than most other clusters.

Cluster 1c includes fentanyl (**30**) and similar amide-chain derivatives. None of the ions strongly characteristic of this cluster have previously been reported. The typical ions of m/z = 146 and 189, are common to analogues of clusters 1b, 1c and 1d, and thus cluster 1c is differentiated by the more specific ions reported in **Table 2**. The most notable ion associated with cluster 1d is the fluorinated tropylium ion at m/z = 109. Some of the other ions, although they have not been characterised, must include the propionyl amide chain, to explain why non-propionyl 4'-fluorinated derivatives fall within cluster 1b, not 1d.

Two of the most important cluster 1e ions, m/z = 136 and 150, have not been characterised, but likely structures, which arise from fragmentation of the piperidine ring, are suggested in **Table 2**. Ions analogous to m/z = 150 were observed in other clusters, with a mass difference consistent with the substituent on the aromatic ring (m/z = 132 for cluster 1c; m/z = 166 for cluster 1h, m/z

= 162 for cluster 1h). The m/z = 275 ion and its 276 isotope are unique to para-fluoro cyclopropylfentanyl (**40**). This seems to be a rare occurrence where an ion from a single compound contributes to defining a cluster, and may be a limitation of cluster 1e.

Cluster 1f, which includes 3-fluorinated derivatives (**41-43**), is characterised mostly by unknown ions. Most common ions of 3-fluorinated compounds also arise in fluoroaniline derivatives (clusters 1e and 1i), because of the position of the fluorine atom, which is retained in major EI-MS fragments. Therefore, the distinction between these clusters is based on differences detected in minor fragments. The ion at m/z = 207 is an exception: it characterises cluster 1f because its intensity in 3-fluorinated derivatives is stronger than in other fluorinated compounds.

Cluster 1g is most strongly characterised by the chlorinated m/z = 223 ion and its 224 and 225 isotopes. As previously discussed, the m/z = 166 ion is suggested to arise from a fragmentation of the piperidine ring. Cluster 1h includes methoxylated derivatives (**47-51**). It is strongly characterised by m/z = 162, as well as m/z = 134 which is consistent with further fragmentation of the piperidine ring. The m/z = 108 ion corresponds to a methoxyphenyl cation, while m/z = 176 and its 177 isotope are the methoxyl equivalent of a known fentanyl fragment. Finally, individuals in cluster 1i are differentiated from other fluorinated compounds in clusters 1e and 1f mostly by m/z = 263, which includes the propionyl amide chain. Cluster 1i is also characterised by common fluorinated fragment m/z = 164.

Table 2. Description of Classifier 1 clusters by the five most significant m/z ions.

Cluster	m/z	Mean in cluster	Overall mean [a]	p-value [b]	Suspected fragment
1a	82	0.816	0.133	1.1E-12	
	91	1.000	0.302	6.0E-12	
	173	0.168	0.026	8.6E-12	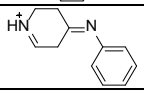
	174	0.070	0.011	8.6E-12	m/z = 173 isotope
	92	0.089	0.039	7.5E-08	m/z = 91 isotope
1b	160	0.179	0.077	9.1E-03	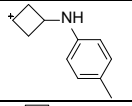
	203	0.086	0.033	1.2E-02	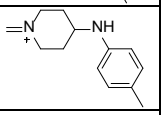
	204	0.018	0.009	1.8E-02	m/z = 203 isotope
	119	0.035	0.025	3.3E-02	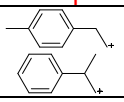
	117	0.037	0.030	3.8E-02	–
1c	104	0.177	0.081	4.5E-06	–
	159	0.027	0.009	4.5E-06	–
	132	0.167	0.076	7.7E-06	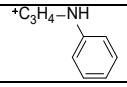
	147	0.087	0.031	8.6E-06	m/z = 146 isotope
	98	0.067	0.023	1.1E-05	–
1d	109	0.197	0.022	6.0E-11	
	101	0.043	0.005	1.5E-09	–
	93	0.529	0.096	7.8E-08	–
	66	0.040	0.011	7.4E-07	–
	103	0.216	0.078	2.4E-06	–
1e	150	0.069	0.018	1.5E-04	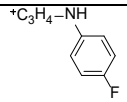
	206	0.070	0.009	5.2E-04	–
	136	0.048	0.015	1.5E-03	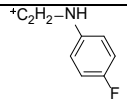
	275	0.200	0.019	1.8E-03	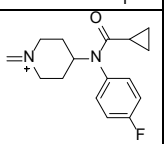
	276	0.036	0.004	1.8E-03	m/z = 275 isotope

Table 2. Description of Classifier 1 clusters by the five most significant m/z ions. (cont.)

Cluster	m/z	Mean in cluster	Overall mean [a]	p-value [b]	Suspected fragment
1f	114	0.060	0.004	3.7E-13	–
	186	0.248	0.034	5.8E-12	–
	207	0.498	0.081	1.5E-06	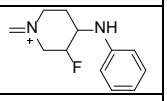
	185	0.035	0.010	1.0E-05	–
	71	0.395	0.044	1.6E-05	–
1g	225	0.122	0.007	4.0E-13	m/z = 223 isotope
	223	0.381	0.022	4.1E-13	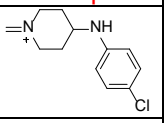
	224	0.056	0.003	5.4E-13	m/z = 223 isotope
	127	0.121	0.007	1.5E-12	–
	166	0.065	0.004	3.9E-12	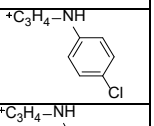
1h	162	0.078	0.010	2.8E-11	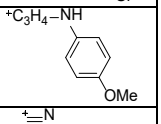
	134	0.094	0.020	7.2E-11	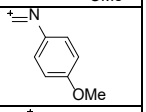
	108	0.100	0.011	1.3E-10	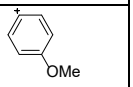 isotope
	176	0.676	0.073	3.2E-10	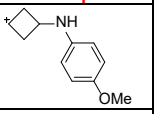
	177	0.106	0.014	8.6E-10	m/z = 176 isotope
1i	111	0.567	0.046	3.1E-12	–
	167	0.066	0.005	5.0E-12	–
	263	1.000	0.075	4.3E-10	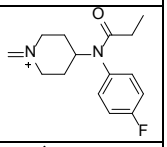
	164	0.668	0.071	6.2E-10	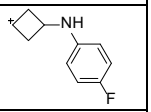
	112	0.039	0.004	8.0E-10	–

[a] Average value for the total dataset; [b] Probability that a variable follows a standard normal distribution.

Cluster 1b poses a problem for the accurate classification of unknown compounds, because it includes analogues from multiple different structural classes. However, further dividing the dendrogram does not lead to more relevant classes (as shown in **Figure S4b**). A potential solution to this problem is to construct a second PCA model, with only compounds from cluster 1b. Any unknown compound grouped with cluster 1b could then be fed into this second model and properly classified through an iterative process. The resulting dendrogram of Classifier 2 is shown in **Figure 6**. A PCA was performed on compounds from cluster 1b and the first four PCs were retained (51.2% of total variance). Four clusters clearly arose from the hierarchical clustering and **Table 3** reports the individual compounds which contribute to each cluster. As opposed to the first classifier, this one allows the proper grouping of fluorophenethyl- (cluster 2a) and methylaniline (cluster 2d) analogues. Cluster 2c includes compounds with aromatic amides which, because of the increased stability of their amide and acylium ions, produce significantly different mass spectra from other amides. Cluster 2b groups two types of compounds. Firstly, aliphatic amides which are uncaptured by Classifier 1 [i.e. 3-tetrahydrofuranyl- (**15**); heptanoyl- (**17**) and 2,2-dimethylpropanoylfentanyl (pivaloylfentanyl, **23**)]. Cluster 2b also includes compounds bearing methyl substituents on their phenethyl- tails, either on the aromatic ring or on the ethyl linker, which are difficult to identify because the resulting fragment ions are not significantly different, in mass or intensity, from those of other analogues. [35]

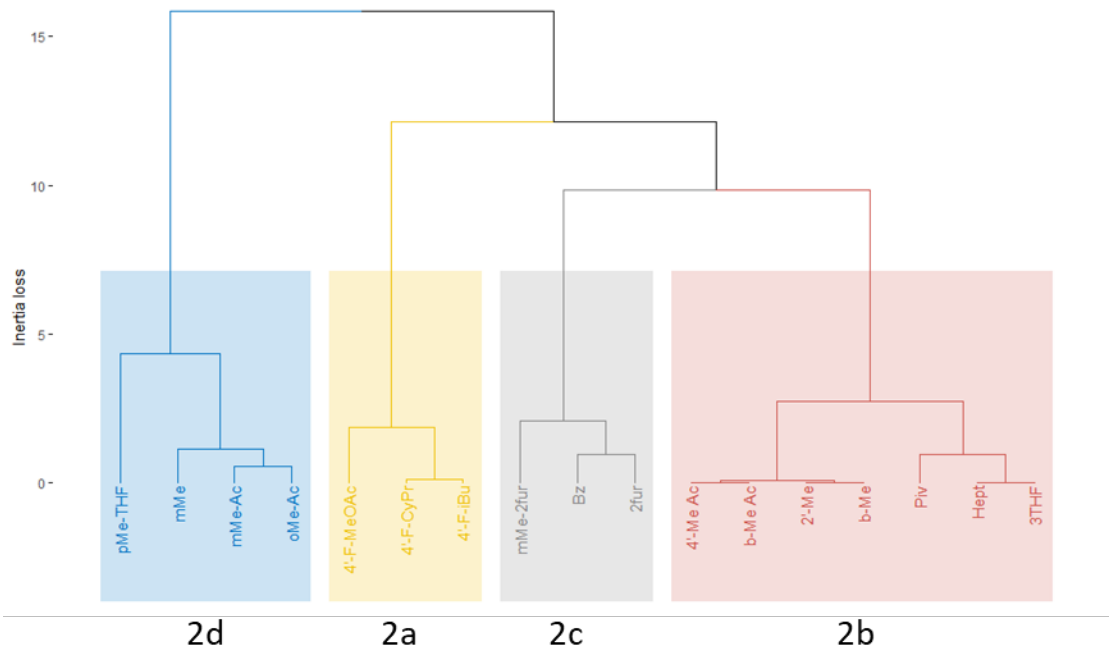

Figure 6. Classifier 2 dendrogram created from the hierarchical clustering of fentanyl analogues.

Note: The vertical axis represents the loss of inertia caused by each grouping.

Table 3. Individuals in each cluster of Classifier 2.

Cluster		Fentanyl analogue	Abbreviation	Nº
1	Fluorophenethyl-	4'-Fluoro-methoxyacetyl-	4'-F-MeOAc	**26**
		4'-Fluoro-cyclopropyl-	4'-F-CyPr	**20**
		4'-Fluoro-butyryl-	4'-F-Bu	**24**
2	Methylphenethyl- & Amides	4'-Methyl-acetyl-	4'-Me Ac	**11**
		Heptanoyl-	Hept	**17**
		β-Methyl-acetyl-	b-Me Ac	**12**
		Tetrahydrofuranyl- (3-isomer)	3THF	**15**
		2'-Methyl-	2'-Me	**13**
		2,2-dimethylpropanoyl-	Piv	**23**
		β-Methyl-	b-Me	**16**
3	Aromatic amides	Benzoyl- (Phenyl)	Bz	**21**
		Furanyl-	2-fur	**25**
		meta-Methyl-furanyl-	mMe-2fur	**18**
4	Methylanilines	meta-Methyl-acetyl-	mMe-Ac	**10**
		para-Methyl-tetrahydrofuranyl-	pMe-THF	**14**
		ortho-Methyl-acetyl-	oMe-Ac	**9**
		meta-Methyl-	mMe	**8**

The most characteristic m/z ions of each Classifier 2 cluster are reported in **Table 4**. Cluster 2a is characterised by a fluorophenethyl cation (m/z = 123) and a fluorinated tropylium fragment (m/z = 109), both characteristic of fentanyl analogues bearing a fluorine on their phenethyl chain. Cluster 2b includes m/z = 146, a typical fentanyl fragment, as well as a methylphenethyl cation (m/z = 119).

The ions reported for cluster 2c do not appear to be common to all three compounds. In this case, it proved more relevant to examine ions with a lower average than the overall dataset. This is because all three compounds have an acylium ion as their base peak, due to the increased stability of their aromatic amide chain (m/z = 95 for 2-furanylfentanyl (**25**) and meta-methylfuranylfentanyl (**18**); m/z = 105 for benzoylfentanyl (**21**)). This decreases the relative intensity of common fragment ions when compared to other analogues. As shown in **Table 4**, m/z = 146 and its 147 isotope, one of the major fragments of fentanyl (**30**), is lower in cluster 2c than in the whole dataset. This explains how aromatic compounds with different fragment ions can still cluster together. Finally, cluster 2d is characterised by m/z = 160 and 203 fragments, which are expected for methylaniline compounds.

Table 4. Description of Classifier 2 clusters by the five most significant m/z values.

Cluster	m/z	Mean in cluster	Overall mean[a]	p-value[b]	Suspected fragment
2a	123	0.174	0.031	6.8E-05	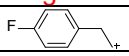
	122	0.073	0.013	8.7E-05	–
	121	0.032	0.007	1.0E-04	–
	109	0.079	0.015	1.1E-04	
	101	0.026	0.006	1.4E-04	–
2b	131	0.049	0.040	2.9E-03	–
	146	0.481	0.298	8.5E-03	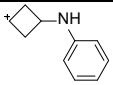
	119	0.059	0.037	3.0E-02	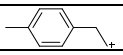
	188	0.124	0.061	3.8E-02	–
	147	0.054	0.038	3.9E-02	m/z = 146 isotope
2c	95	0.669	0.138	1.8E-03	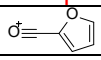
	98	0.056	0.018	3.6E-03	–
	184	0.034	0.012	1.7E-02	–
	294	0.022	0.004	2.4E-02	m/z = 293 isotope
	293	0.103	0.019	2.4E-02	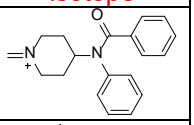
	146	0.028	0.298	3.2E-02	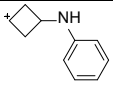
	131	0.028	0.040	2.8E-02	–
	147	0.005	0.038	2.0E-02	m/z = 146 isotope
	132	0.039	0.087	8.3E-04	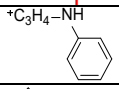
2d	160	0.791	0.197	1.2E-04	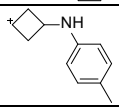
	161	0.103	0.027	1.8E-04	m/z = 160 isotope
	145	0.074	0.026	2.2E-04	–
	144	0.082	0.032	4.9E-04	–
	203	0.387	0.096	6.0E-04	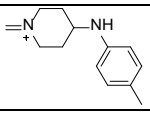

[a] Average value for the total dataset; [b] Probability that a variable follows a standard normal distribution.

3.3 Model evaluation

An in-silico evaluation of the proposed model was performed using the remaining 67 fentanyl analogues. A given test point is projected in the PCA space, and the distance between this point and every cluster is calculated. A test sample can be matched to the specific cluster with the nearest centroid, or to the cluster of its nearest neighbour. These two match criteria were compared in terms of accuracy, as reported in **Table 5**. The nearest neighbour method, which correctly classified 61 of the 67 test compounds, was more accurate overall (91.0% accuracy).

Table 5. Comparison of the centroid and nearest neighbour classification criteria. [a] Compounds classed in cluster 2 excluded.

	Centroid method	Nearest neighbour method
Classifier 1 matches[a]	37 / 43	37 / 39
Classifier 2 matches	19 / 24	24 / 28
Total matches	56 / 67	61 / 67
Overall accuracy	83.6%	91.0%

The detailed results obtained using the nearest neighbour method are reported in the Supplementary Information (**Table S3**). Expected clusters, based on an individual's structural class, are also reported in **Table S3** as a match criterion.

Overall, Classifier 1 reliably identified a variety of N-benzyl derivatives (cluster 1a), most aliphatic amides (cluster 1c), fluoroaniline derivatives (cluster 1e), chloroaniline derivatives (cluster 1g). It also properly classified 3-fluoro-isobutyrylfentanyl (**114**) in cluster 1f and para-methoxy-butyrylfentanyl (**120**) in cluster 1h, though these classes only had a limited number of compounds to test. Interestingly, fluoroaniline compounds bearing an aromatic amide chain (**111-112**) were classed in cluster 1e rather than 1b, meaning that the acylium ion contributed less to clustering than in other classes.

Misclassifications made by Classifier 1 involved aromatic amides 2,3-benzodioxolefentanyl (**108**) and para-chloro-2-furanylfentanyl (**109**), wrongly classed in cluster 1e. Compound **108** shows a

base peak at m/z = 149, associated with its acylium ion, accompanied with a ^{13}C isotope at m/z = 150 (8.7% relative intensity). Coincidentally, a peak at m/z = 150 with a similar intensity occurs in most fluoroaniline derivatives and happens to be strongly characteristic of compounds in cluster 1e (see **Table 2**), which can explain the misclassification. The main reason for the misclassification of **109** lies in the fact that it projects very low on PC3 as opposed to other chloroaniline derivatives, which are mostly characterised by strong m/z = 223, 224 and 225 ions. In **109**, the relative intensity of these fragments is significantly decreased because of the strong m/z = 95 acylium ion (base peak).

Compounds in cluster 1b were screened against Classifier 2, which properly identified methylaniline (cluster 2d) and 4'-fluoro (cluster 2a) derivatives. As cluster 2b includes methylphenethyl- and non-aromatic amide derivatives, test individuals in cluster 2b were tentatively classified into one of these two classes based on their nearest neighbour. This led to the proper sub-classification of 8 compounds (**65-68**, **82-84**, **88**) originally included in cluster 2b, and the misclassification of 4-ANPP (**64**), α-Methyl-butyrylfentanyl (**85**) and α-Methyl-fentanyl (**86**). 4-ANPP (**64**) does not bear an amide chain, but it might have been expected to cluster in either 1c or 2b, considering it shares major m/z ions with fentanyl. Although Classifer 2 had limitations, this could be solved by including more derivatives from each class in the model, which was not possible with the current dataset.

As noted previously, aromatic amides tend to cluster together in the classifier 2 model. Aromatic amides tested were thus classed in cluster 2c, regardless of other modifications to their structure (chlorinated, methoxylated and methylated analogues). Again, this could be remediated by adding aromatic compounds representative of each class of derivatives to the model. In fact, an initial exploration using all aromatic compounds available in the full dataset shows that they can cluster based on their secondary modification (see **Figure 7**). The partition is not perfect, with furanylfentanyl (**25**) clustering on its own, but could be improved by including more examples of this class of derivatives.

Additionally, compounds **5-6**, **21**, **25**, **28-32**, **34**, **40**, **58** and **62**, which were synthesised and analysed in-house, were also available on the SWGDRUG library. The SWGDRUG spectra were analysed with the model to evaluate the possible variability when the same compounds are injected on different instruments (see Table S3). Of the 13 compounds tested, 9 were classed in exactly the

same cluster. Four amide derivatives (**28-29**, **31-32**) were classed in cluster 1b, due to differences in peak intensities on the different instruments. When analysed with Classifier 2, however, all four compounds were classed in the "amides" cluster (cluster 2b). This indicates that the use of both classifiers mitigates the effect of intra-injection variability.

Although this model allows the classification of fentanyl analogues, it does not allow the discrimination of regioisomers, which produce the same mass ions (e.g. ortho-, meta- and para-compounds). However, separation of fluorofentanyl regioisomers has been achieved by Bonetti using PCA followed by linear discriminant analysis on multiple injections of the same compounds. [21] Potentially, the model presented in this paper, could be applied in conjunction with Bonetti's approach. The present model could "triage" unknown fentalogues, to identify their "class" and subsequently Bonetti's model could be applied in conjunction to confirm/validate the class and subsequently determine the position of a substituent.

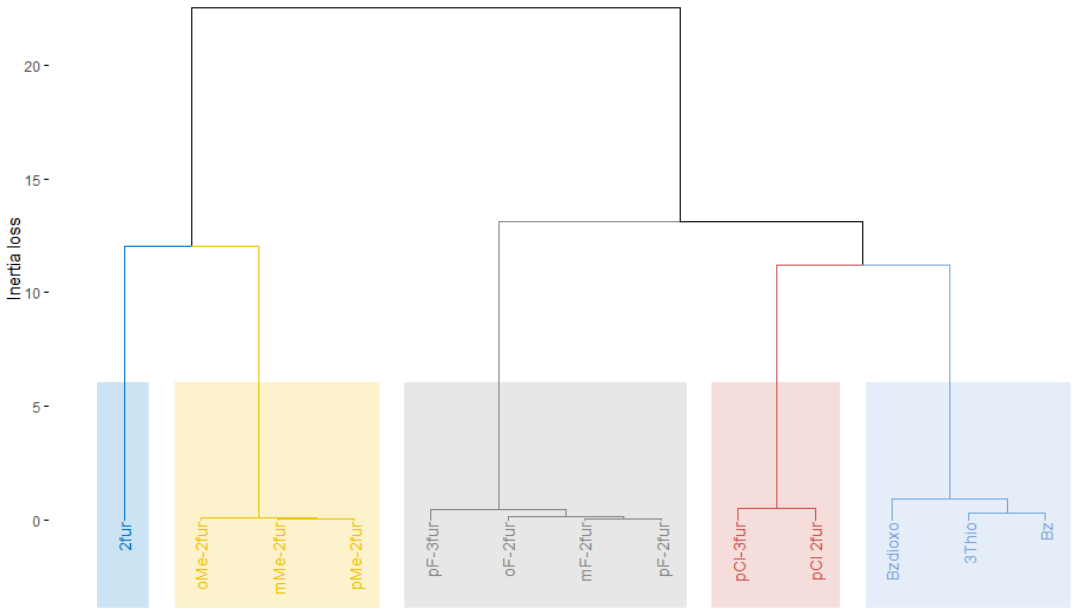

Figure 7. Dendrogram created from the hierarchical clustering of aromatic amide analogues. Note: The vertical axis represents the loss of inertia caused by each grouping.

4. Conclusion

In conclusion, a principal component analysis (PCA) and hierarchical clustering model was used to classify fentanyl analogues with high accuracy. The model can be used to aid the structural elucidation of novel fentanyl analogues encountered in forensic casework. It can automatically identify the structural class of unknown fentanyl derivatives based on their EI-MS spectra. The model is more precise than previously described spectral mapping models, because the PCA forms clusters based on the intensity of specific fragments rather than shifts in spectral peaks. [24] For instance, all ortho-, meta- and para-fluorinated compounds project close to each other in the PCA space, because fluorination of the aniline ring of fentanyl leads to very specific fragments shared by these analogues. Rather than only detect a modification of the aniline ring, the classifier was thus able to detect what modification was introduced. This model works reliably with compounds that are two modifications away from fentanyl, because it was constructed using many examples of these types of compounds. One drawback is that the model relies on the availability of enough spectra of representative analogues for classes to arise.

Funding

This work was supported by the Natural Sciences and Engineering Research Council of Canada [396154510]; the Fonds de Recherche du Québec—Nature et Technologie [206375]; and Manchester Metropolitan University.

Declaration of interests

The authors declare that they have no known competing financial interests or personal relationships that could have appeared to influence the work reported in this paper.

References

[1] J. Mounteney, I. Giraudon, G. Denissov, P. Griffiths. Fentanyls: Are we missing the signs? Highly potent and on the rise in Europe, Int J Drug Policy. 26 (2015) 626-631. http://10.1016/j.drugpo.2015.04.003

[2] J. Suzuki, S. El-Haddad. A review: Fentanyl and non-pharmaceutical fentanyls, Drug Alcohol Depend. 171 (2017) 107-116. Http://doi.org/10.1016/j.drugalcdep.2016.11.033

[3] P. Armenian, K. T. Vo, J. Barr-Walker, K. L. Lynch. Fentanyl, fentanyl analogs and novel synthetic opioids: A comprehensive review, Neuropharmacology (2017). 10.1016/j.neuropharm.2017.10.016

[4] L. Scholl, P. Seth, M. Kariisa, N. Wilson, G. Baldwin. Drug and opioid-involved overdose deaths — United States, 2013–2017, MMWR Morb Mortal Wkly Rep. 67 (2019) 1419–1427. http://dx.doi.org/10.15585/mmwr.mm675152e1

[5] S. N. Lucyk, L. S. Nelson. Novel Synthetic Opioids: An Opioid Epidemic Within an Opioid Epidemic, Ann Emerg Med. 69 (2017) 91-93. http://doi.org/10.1016/j.annemergmed.2016.08.445

[6] P. Armenian, A. Olson, A. Anaya, A. Kurtz, R. Ruegner, R. R. Gerona. Fentanyl and a Novel Synthetic Opioid U-47700 Masquerading as Street "Norco" in Central California: A Case Report, Ann Emerg Med. 69 (2017) 87-90. http://doi.org/10.1016/j.annemergmed.2016.06.014

[7] L. Hikin, P. R. Smith, E. Ringland, S. Hudson, S. R. Morley. Multiple fatalities in the North of England associated with synthetic fentanyl analogue exposure: Detection and quantitation a case series from early 2017, Forensic Sci Int. 282 (2018) 179-183. http://doi.org/10.1016/j.forsciint.2017.11.036

[8] P. J. Jannetto, A. Helander, U. Garg, G. C. Janis, B. Goldberger, H. Ketha. The Fentanyl Epidemic and Evolution of Fentanyl Analogs in the United States and the European Union, Clin Chem. 65 (2019) 242-253. http://doi.org/10.1373/clinchem.2017.281626

[9] Advisory Council on the Misuse of Drugs, Misuse of fentanyl and fentanyl analogues. https://assets.publishing.service.gov.uk/government/uploads/system/uploads/attachment_data/file/855893/ACMD_Report_-_Misuse_of_fentanyl_and_fentanyl_analogues.pdf, 2020 (accessed 15 Jan 2020).

[10] United Nations Office on Drugs and Crime, January 2020 – United Kingdom: ACMD report on the misuse of fentanyl and fentanyl analogues as global number of opioid NPS rises. https://www.unodc.org/LSS/Announcement/Details/94dc6286-16bb-4e7a-9429-65d28918b332, 2020 (accessed 15 July 2020).

[11] J. M. Stogner. The potential threat of acetyl fentanyl: legal issues, contaminated heroin, and acetyl fentanyl "disguised" as other opioids, Ann Emerg Med. 64 (2014) 637-639. https://doi.org/10.1016/j.annemergmed.2014.07.017

[12] F. Bravo, D. Gonzalez, J. Benites. Development and validation of a solid-phase extraction gas chromatography-mass spectrometry method for the simultaneous quantification of opioid drugs in human whole blood and plasma, J Chil Chem Soc. 56 (2011) 799-802.

[13] S. Strano-Rossi, I. Alvarez, M. J. Tabernero, P. Cabarcos, P. Fernandez, A. M. Bermejo. Determination of fentanyl, metabolite and analogs in urine by GC/MS, J Appl Toxicol. 31 (2011) 649-654. 10.1002/jat.1613

[14] N. Misailidi, S. Athanaselis, P. Nikolaou, M. Katselou, Y. Dotsikas, C. Spiliopoulou, I. Papoutsis. A GC–MS method for the determination of furanylfentanyl and ocfentanil in whole blood with full validation, Forensic Toxicol. 37 (2019) 238-244. http://doi.org/10.1007/s11419-018-0449-2

[15] N. Gilbert, L. H. Antonides, C. J. Schofield, A. Costello, B. Kilkelly, A. R. Cain, P. R. V. Dalziel, K. Horner, R. E. Mewis, O. B. Sutcliffe. Hitting the Jackpot – development of gas chromatography–mass spectrometry (GC–MS) and other rapid screening methods for the analysis of 18 fentanyl-derived synthetic opioids, Drug Test Anal. 12 (2020) 798-811. http://doi.org/10.1002/dta.2771

[16] H. Abdi, L. J. Williams. Principal component analysis, WIREs Comp Stats. 2 (2010) 433-459. https://10.1002/wics.101

[17] B. P. Mayer, A. J. DeHope, D. A. Mew, P. E. Spackman, A. M. Williams. Chemical Attribution of Fentanyl Using Multivariate Statistical Analysis of Orthogonal Mass Spectral Data, Anal Chem. 88 (2016) 4303-4310. https://10.1021/acs.analchem.5b04434

[18] J. Omar, B. Slowikowski, C. Guillou, F. Reniero, M. Holland, A. Boix. Identification of new psychoactive substances (NPS) by Raman spectroscopy, J Raman Spectrosc. 50 (2019) 41-51. https://doi.org/10.1002/jrs.5496

[19] R. F. Kranenburg, D. Peroni, S. Affourtit, J. A. Westerhuis, A. K. Smilde, A. C. van Asten. Revealing hidden information in GC–MS spectra from isomeric drugs: Chemometrics based identification from 15 eV and 70 eV EI mass spectra, Forensic Chem. 18 (2020) 100225. https://doi.org/10.1016/j.forc.2020.100225

[20] M. P. Levitas, E. Andrews, I. Lurie, I. Marginean. Discrimination of synthetic cathinones by GC–MS and GC–MS/MS using cold electron ionization, Forensic Sci Int. 288 (2018) 107-114. https://doi.org/10.1016/j.forsciint.2018.04.026

[21] J. Bonetti. Mass spectral differentiation of positional isomers using multivariate statistics, Forensic Chem. 9 (2018) 50-61. https://doi.org/10.1016/j.forc.2018.06.001

[22] J. T. Davidson, G. P. Jackson. The differentiation of 2,5-dimethoxy-N-(N-methoxybenzyl)phenethylamine (NBOMe) isomers using GC retention indices and multivariate analysis of ion abundances in electron ionization mass spectra, Forensic Chem. 14 (2019) 100160. https://doi.org/10.1016/j.forc.2019.100160

[23] A. L. Setser, R. Waddell Smith. Comparison of variable selection methods prior to linear discriminant analysis classification of synthetic phenethylamines and tryptamines, Forensic Chem. 11 (2018) 77-86. https://doi.org/10.1016/j.forc.2018.10.002

[24] A. S. Moorthy, A. J. Kearsley, W. G. Mallard, W. E. Wallace. Mass spectral similarity mapping applied to fentanyl analogs, Forensic Chem. 19 (2020) 100237. https://doi.org/10.1016/j.forc.2020.100237

[25] C. A. Valdez, R. N. Leif, B. P. Mayer. An efficient, optimized synthesis of fentanyl and related analogs, PloS One. 9 (2014) e108250. http://doi.org/10.1371/journal.pone.0108250

[26] V. Spahn, G. Del Vecchio, D. Labuz, A. Rodriguez-Gaztelumendi, N. Massaly, J. Temp, V. Durmaz, P. Sabri, M. Reidelbach, H. Machelska, M. Weber, C. Stein. A nontoxic pain killer designed by modeling of pathological receptor conformations, Science. 355 (2017) 966-969. http://doi.org/10.1126/science.aai8636

[27] M. Schönberger, D. Trauner. A Photochromic Agonist for μ-Opioid Receptors, Angew Chem Int Ed. 53 (2014) 3264-3267. http://doi.org/10.1002/anie.201309633

[28] Scientific Working Group for the Analysis of Seized Drugs, SWGDRUG MS Library Version 3.7. http://www.swgdrug.org/ms.htm, 2020 (accessed 17 June 2020).

[29] F. Husson, J. Josse, S. Lê. FactoMineR: An R Package for Multivariate Analysis, J Stat Softw. 25 (2008). https://doi.org/10.18637/jss.v025.i01

[30] A. Kassambara, F. Mundt, factoextra: Extract and Visualize the Results of Multivariate Data Analyses. R package version 1.0.6. https://CRAN.R-project.org/package=factoextra, 2019 (accessed 17 June 2020).

[31] A. Kassambara, Practical guide to cluster analysis in R: Unsupervised machine learning, STHDA, 2017.

[32] R. Tibshirani, G. Walther, T. Hastie. Estimating the number of clusters in a data set via the gap statistic, J R Stat Soc B. 63 (2001) 411-423. https://doi.org/10.1111/1467-9868.00293

[33] L. Kaufman, P. Rousseeuw, Finding Groups in Data: An Introduction to Cluster Analysis, 2009.

[34] H. G. Pierzynski, L. Neubauer, C. Choi, R. Franckowski, S. D. Augustin, D. M. Iula. Tips for interpreting GC-MS fragmentation of unknown substituted fentanyls, Cayman Currents. 28 (2017) 1-3.

[35] H. Ohta, S. Suzuki, K. Ogasawara. Studies on Fentanyl and Related Compounds IV. Chromatographic and Spectrometric Discrimination of Fentanyl and its Derivatives, J Anal Toxicol. 23 (1999) 280-285. https://doi.org/10.1093/jat/23.4.280